Title	Bipolar disorder and gender are associated with frontolimbic and basal ganglia dysconnectivity: A study of topological variance using network analysis
Author(s)	Nabulsi, Leila; McPhilemy, Genevieve; Kilmartin, Liam; O'Hora, Denis; O'Donoghue, Stefani; Forcellini, Giulia; Najt, Pablo; Ambati, Srinath; Costello, Laura; Byrne, Fintan; McLoughlin, James; Hallahan, Brian; McDonald, Colm; Cannon, Dara M.
Publication Date	2019-12-16
Publication Information	Nabulsi, Leila, McPhilemy, Genevieve, Kilmartin, Liam, O'Hora, Denis, O'Donoghue, Stefani, Forcellini, Giulia, Najt, Pablo, Ambati, Srinath, Costello, Laura, Byrne, Fintan, McLoughlin, James, Hallahan, Brian, McDonald, Colm, Cannon, Dara M. (2019). Bipolar Disorder and Gender Are Associated with Frontolimbic and Basal Ganglia Dysconnectivity: A Study of Topological Variance Using Network Analysis. Brain Connectivity, 9(10), 745-759. doi:10.1089/brain.2019.0667
Publisher	Mary Ann Liebert
Link to publisher's version	https://doi.org/10.1089/brain.2019.0667
Item record	http://hdl.handle.net/10379/16008
DOI	http://dx.doi.org/10.1089/brain.2019.0667

- **For citation please use: Brain Connect. 2019 Dec;9(10):745-759. doi: 10.1089/brain.2019.0667. PMID: 31591898**

Title Page

Bipolar Disorder and Gender are Associated with Fronto-limbic and Basal Ganglia Dysconnectivity: A Study of Topological Variance Using Network Analysis

Authors: Leila Nabulsi[1], Genevieve McPhilemy[1], Liam Kilmartin[2], Denis O'Hora[3], Stefani O'Donoghue[1], Giulia Forcellini[1,4], Pablo Najt[1], Srinath Ambati[1], Laura Costello[1], Fintan Byrne[1], James McLoughlin[1], Brian Hallahan[1], Colm McDonald[1], Dara M. Cannon[1]

Affiliations:[1]Centre for Neuroimaging & Cognitive Genomics (NICOG), Clinical Neuroimaging Laboratory, NCBES Galway Neuroscience Centre, College of Medicine, Nursing, and Health Sciences, National University of Ireland Galway, H91 TK33 Galway, Ireland; [2]College of Engineering and Informatics, National University of Ireland Galway, Galway, Ireland; [3]School of Psychology, National University of Ireland Galway, Galway, Ireland; [4]Center for Neuroscience and Cognitive Systems, Istituto Italiano di Tecnologia, Rovereto (TN), Italy.

E-mail addresses in order of Authorship:

Leila Nabulsi - l.nabulsi1@nuigalway.ie

Genevieve McPhilemy - g.mcphilemy1@nuigalway.ie

Liam Kilmartin - liam.kilmartin@nuigalway.ie

Denis O'Hora - denis.ohora@nuigalway.ie

Stefani O'Donoghue - stefani.odonoghue@gmail.com

Giulia Forcellini - giuliafor.91@gmail.com

Pablo Najt - pablonajt@hotmail.com

Srinath Ambati - srinathambati@gmail.com

Laura Costello - l.costello9@nuigalway.ie

Fintan Byrne – fintan.byrne@hse.ie

James McLoughlin - james.McLoughlin@hse.ie

Brian Hallahan - brian.hallahan@nuigalway.ie

Colm McDonald - colm.mcdonald@nuigalway.ie

Dara M. Cannon - dara.cannon@nuigalway.ie

Corresponding Author: Leila Nabulsi, The Centre for Neuroimaging & Cognitive Genomics (NICOG), Clinical Neuroimaging Lab, NCBES Galway Neuroscience Centre, College of Medicine, Nursing, and Health Sciences, National University of Ireland Galway, H91 TK33 Galway, Ireland

Email address: l.nabulsi1@nuigalway.ie

Telephone number: +353 91495465

Fax number: N/A

Running head: Basal Ganglia & Fronto-limbic Connectivity in BD

Keywords: Bipolar disorder, Graph Theory, Basal Ganglia, Fronto-limbic, Rich-club, Gender.

Abstract

Well-established structural abnormalities, mostly involving the limbic system, have been associated with disorders of emotion regulation. Understanding the arrangement and connections of these regions with other functionally specialized cortico-subcortical subnetworks is key to understanding how the human brain's architecture underpins abnormalities of mood and emotion. We investigated topological patterns in bipolar disorder (BD) with the anatomically improved precision conferred by combining subject-specific parcellation/segmentation with non-tensor based tractograms derived using a high-angular resolution diffusion-weighted approach.

Connectivity matrices were constructed using 34-cortical and 9-subcortical bilateral nodes (Desikan-Killiany) and edges that were weighted by fractional anisotropy and streamline count derived from deterministic tractography using constrained spherical deconvolution. Whole-brain and rich-club connectivity alongside a permutation-based statistical approach were employed to investigate topological variance in predominantly euthymic BD relative to healthy volunteers.

Bipolar disorder patients (n=40) demonstrated impairments across whole-brain topological arrangements (density, degree, and efficiency), and a dysconnected subnetwork involving limbic and basal ganglia relative to controls (n=45). Increased rich-club connectivity was most evident in females with BD, with fronto-limbic and

parieto-occipital nodes not members of BD rich-club. Increased centrality in females relative to males was driven by basal ganglia and fronto-temporo-limbic nodes.

Our subject-specific cortico-subcortical non-tensor-based connectome map presents a neuroanatomical model of BD dysconnectivity that differentially involves communication within and between emotion-regulatory and reward-related subsystems. Moreover, the female brain positions more dependence on nodes belonging to these two differently specialised subsystems for communication relative to males, which may confer increased susceptibility to processes dependent on integration of emotion and reward-related information.

Acronyms

Analysis of Covariance (ANCOVA)

Anterior Limb of the Internal Capsule (ALIC)

Automated Anatomical Labelling Atlas (AAL)

Bipolar disorder (BD)

Characteristic Path Length (L)

Clustering Coefficient (CC)

Constrained Spherical Deconvolution tractography (CSD)

Default Mode Network (DMN)

Diagnostic and Statistical Manual of Mental Disorders, 4th edition (DSM -IV)

Diffusion Tensor Imaging (DTI)

Echo Time (TE)

Family-wise error rate (FWER)

Field Of View (FOV)

Fractional Anisotropy (FA)

Global Efficiency (E_g)

Hamilton Anxiety Rating scale (HARS)

Hamilton Depression Rating Scale (HDRS-21)

High Angular Resolution Diffusion Imaging (HARDI)

Left Hemisphere (lh)

Magnetic Resonance Imaging (MRI)

Magnetization-prepared Rapid Gradient-echo (MPRAGE)

Mean Diffusivity (MD)

Multivariate Analysis of Covariance (MANCOVA)

Network-based Statistics (NBS)

Number of Streamlines (NOS)

Repetition Time (TR)

Right Hemisphere (rh)

Streamline Density (SD)

Tract-based Spatial Statistics (TBSS)

Voxel-based Analysis (VBA)

Young Mania Rating Scale (YMRS)

Introduction

Bipolar disorder (BD) affects approximately 1-3% of the population (Merikangas et al., 2011) and is characterised by intermittent episodes of depression and (hypo)mania proposed to be due to dysconnectivity within the illness brain circuitries. Although the underlying neurobiology of BD remains unclear, there is evidence for distinctive anatomical and functional patterns of abnormalities in the neural system involving emotion and reward-related circuitries (Perry et al., 2018; Blond et al., 2012; Strakowski et al., 2012), that may elucidate functional impairments of the illness. However, due to substantial heterogeneity across the literature a structural neuroanatomical pattern of BD using protocols of magnetic resonance imaging (MRI) has yet to be fully defined and understood. The partial overlap in symptoms and neuroanatomical abnormalities for bipolar and other mood disorders emphasises the need for a deeper understanding of the different neurobiological mechanisms that characterise these disorders. This is key to identifying novel and tailored treatment targets in order to improve life quality of patients suffering from BD.

Tensor-based diffusion imaging (DTI) studies have implicated white matter deficits in major fibres carrying impulses to and from the cortical areas that regulate emotional, cognitive and behavioural aspects of the illness (reviewed in Nortje et al., 2013; Vederine et al., 2011; Emsell & McDonald, 2009). These findings suggest that changes in BD extend beyond the white matter microstructural organization of fronto-limbic connections that support emotion regulation in the brain to include posterior and interhemispheric projections. Additionally, deficits in grey matter measures have been reported across cortico-subcortical regions in BD with the strongest effects seen

across frontal and inferior temporal cortices and limbic system structures, with associations identified for illness duration and medication exposure (Hibar et al., 2017, 2016; Hallahan et al., 2011). However, there are inconsistencies amongst DTI and grey matter volumetric studies on the anatomical location and direction of findings.

With the aim to investigate BD connectivity using a more anatomically comprehensive approach, structural and diffusion MRI scans can be combined together in connectome analyses to extend beyond focal grey and white matter investigations that would be provided by examining structural and diffusion scans alone. This approach of network analysis allows for brain circuits to be represented in a network-like pattern using the science of complex networks – graph theory – whereby grey matter regions are represented as 'nodes' and their axonal bundles linking these nodes as 'edges'. By mapping the brain as a graph, topological features of a network can be inferred to describe features of integration and segregation at the whole-brain and nodal level. This has facilitated investigation of neurobiological changes and consequent cognitive impairments of psychiatric illnesses such as BD (O'Donoghue et al., 2015).

Bipolar disorder has been increasingly considered a 'dysconnection syndrome' as a result of the complex interplay between grey and white matter components involving emotion regulatory circuitries (O'Donoghue et al., 2017a). Although scarce, structural connectivity analyses in BD (reviewed elsewhere (O'Donoghue et al., 2017a), Table 1) presented disrupted whole-brain integration, left-right decoupling and dysconnectivity of the brain's fronto-limbic and posterior neuroanatomical circuits underpinning emotional dysregulation (O'Donoghue et al., 2017b; Collin et al., 2016; Forde et al., 2015; Gadelkarim et al., 2014; Leow et al., 2013). Disrupted whole-brain

integration is consistent with widespread anisotropy reductions seen in BD (Nortje et al., 2013; Vederine et al., 2011; Emsell & McDonald, 2009). Furthermore, connectivity of centrally located brain regions (hubs) responsible for global integration and coordination of higher cognitive processes within the brain appears preserved (Roberts et al., 2018; Wang et al., 2018; O'Donoghue et al., 2017b; Collin et al., 2016), with evidence of altered rich-club membership in BD (Table 1).

Functional connectivity studies support these anatomical changes in BD, reporting stability of large-scale resting-state networks and regional dysconnectivity mostly involving amygdala, thalamus, anterior cingulate and pre-frontal cortices, alongside abnormalities involving default-mode and fronto-parietal networks in BD (Perry et al., 2018; Syan et al., 2018; Wang et al., 2017; Ajilore et al., 2015; Anand et al., 2009). Functional analyses in BD have been informative, though they have restricted their *a priori* observations to local patterns of connectivity. A preferential pattern of neuroanatomical dysconnectivity has yet to be defined for BD, and it remains unclear whether the illness' impairments result from uniform widespread changes in network topology or if these are just the result from abnormalities within specified subnetworks (Perry et al., 2018). The precise relationship between neuroanatomical changes and functional deficits is unclear (Friston, 2011), and investigation of the structural substrate underpinning BD dysconnectivity may elucidate distinctive neuroanatomical patterns underpinning the disorder and contribute towards a greater understanding of its aetiology and functional impairments.

Despite today's advances in anatomical network reconstruction *in vivo*, obtaining an optimum trade-off between sensitivity and specificity remains challenging (Zalesky et

al., 2016); however, the balance between these must be sought if macroscale mapping of the brain is to be anatomically meaningful and useful in deriving reliable measures of topological organisation. At present, nodal definition for connectivity studies remains unresolved (Zalesky et al., 2016). Studies have availed of a common template (e.g. Automated Anatomical Labelling Atlas, AAL), namely an identical cortico-subcortical parcellation scheme across all subjects (Roberts et al., 2018; Wang et al., 2018; O'Donoghue et al., 2017b; Forde et al., 2015) which reduces inter-subject anatomical variability and although reproducible lacks anatomical accuracy. Subject-specific parcellation schemes such as FreeSurfer (Fischl, 2012) may improve anatomical accuracy of findings by accounting for individual coordinates and volumes. However, studies that have employed subject-specific node definition have limited their observation to cortico-cortical mapping (Collin et al., 2016; Gadelkarim et al., 2014) or regions of interest (Ajilore et al., 2015; Leow et al., 2013). The established importance of the limbic system in BD argues for the inclusion of cortico-subcortical connections in the analyses.

Heterogeneity of findings across structural connectivity studies in BD is largely influenced by the tractography algorithms employed to reconstruct axonal fibre bundles (Bastiani et al., 2012). Connectome sensitivity can be substantially increased by employing algorithms accounting for crossing fibres within a voxel (Tournier et al., 2007). Although deterministic approaches have been recently shown to be well suited for reconstructions of fibre complexity in vivo diffusion MRI, comparisons between different tractography approaches (probabilistic versus deterministic) at mapping connectomes highlight the trade-off between sensitivity and specificity in connectome reconstruction (Sarwar et al., 2018).

With our connectome approach (Figure 1) we explored the topology of previously implicated neuroanatomical dysconnectivity in BD while comparing connectivity across both cortical and subcortical regions and connections involving complex fibre arrangements relative to controls. We examined whole-brain connectivity, most connected subsections of the network (rich-club) and used a statistical approach (Network-based Statistics) to describe the topological arrangement, features of integration and connectivity strength of BD networks. We anticipate that individuals with BD, relative to psychiatrically-healthy controls, will exhibit changes in whole-brain structural connectivity measures and aberrant patterns of structural connectivity involving specified subsystems that implicate nodes belonging to emotion-regulatory circuits systems as previously highlighted by the literature (Perry et al., 2018). With this study we sought both to shed light on BD neuroanatomical deficits and to develop the application of graph theory metrics in psychiatry research.

Methods

Participants

This analysis is based on an independent sample from the previously published bipolar study from our research group (O'Donoghue et al., 2017b), with a small overlap between controls (N=13) and patients (N=6, 15%). Participants, aged 18-65, were recruited by referral or public advertisement from the western regions of Ireland's Health Services. A diagnosis of BD was confirmed using the Diagnostic and Statistical Manual of Mental Disorders (DSM-IV-TR) Structured Clinical Interview for DSM Disorders (American Psychiatric Association, 1994) conducted by an experienced psychiatrist. Mood and anxiety symptoms severity was assessed using the Hamilton Depression (HDRS-21), Anxiety (HARS), and Young Mania (YMRS) Rating Scales at MRI scanning, and in BD a diagnosis of euthymia was defined by HDRS<8, YMRS<7 and HARS<18 scores. Exclusion criteria included neurological disorders, learning disability, comorbid misuse of substances/alcohol and of other Axis-1 disorders, history of head injury resulting in loss of consciousness for >5 minutes along with a history of oral steroid use in the previous 3 months. Healthy controls had no personal history of a psychiatric illness or history among first-degree relatives, defined using the Structured Clinical Interview for DSM-IV Non-patient edition (American Psychiatric Association, 1994). Ethical approval was granted by the University College Hospital Galway Clinical Research Ethics Committee. Participants gave written fully informed consent before participating.

Image Acquisition & Processing

MRI scanning was performed at the Welcome Trust Health Research Board National Centre for Advanced Medical Imaging (CAMI) at St. James's Hospital Dublin, Ireland, using a 3 Tesla Achieva scanner (Philips, The Netherlands). High-resolution 3D T1-weighted turbo field echo magnetization-prepared rapid gradient-echo (MPRAGE) sequence was acquired using an eight-channel head coil (parameters: TR/TE=8.5/3.046 ms, 1 mm^3 isotropic voxel size). Diffusion-weighted images were acquired at b=1200 s/mm^2 along with a single non-diffusion weighted image (b=0), using high angular resolution diffusion imaging (HARDI) involving 61 diffusion gradient directions, 1.8x1.8x1.9 mm voxel dimension and field of view (FOV) 198x259x125 mm. Structural MR images were visually inspected before/after processing for accuracy of cortico-subcortical parcellation and segmentation inspecting grey/white matter boundaries. A probabilistic approach was used to map subject-specific cortico-subcortical brain networks – 34 cortical and 9 subcortical brain regions bilaterally including cerebellum (FreeSurfer v5.3.0; Fischl, 2012) based on the Desikan-Killiany Atlas (Desikan et al., 2006) given any T1-weighted image, for a total of 86 regions.

Diffusion MR images were corrected for subject motion including rotating the b-matrix and eddy-current distortions (ExploreDTI v4.8.6; Leemans et al., 2009). Diffusion images were inspected for potential artefacts, subject head motion, signal dropout, eddy-current induced distortion and partial volume effects. To account for crossing fibres within voxels, we employed a deterministic (non-tensor) constrained spherical (L_{max}=6) deconvolution algorithm (CSD, ExploreDTI v4.8.6; Jeurissen et al., 2014; Tournier et al., 2007). Diffusion eigenvector estimation was performed using the RESTORE approach (Chang et al., 2005). Fibre tracking commenced in each voxel and continued with 1 mm step size, 2 mm^3 seed point resolution, >30° angle curvature

threshold, 20-300 mm length and terminated at a minimum fractional anisotropy (FA) of 0.2.

Structural Connectome Matrices

Whole-brain tractography maps were subsequently used with the parcellated T1 (labels) to generate individual (86x86) undirected connectivity matrices (Figure 1; ExploreDTI v4.8.6). Connectivity matrices were weighted by FA, representing the average FA between two nodes in the network, and by number of streamlines (NOS) representing the number of reconstructed trajectories between two nodes.

Global Measures Derived from the Connectome

Global parameters summarising whole-brain connectivity properties of BD networks were derived from unweighted and weighted matrices and including global density, characteristic path length, global efficiency, global degree/strength, clustering coefficient, calculated as the mean of the respective 86 regional estimates. Furthermore, a global measure of influence and centrality, global betweenness, was investigated (BrainConnectivityToolbox v1.52; Rubinov, 2010). Statistical analysis of whole-brain measures was carried out using multivariate analysis of covariance tests (MANCOVA) with the fixed factors including diagnosis and gender, co-varying for age (IBM SPSS v23).

Statistical Analysis of the Structural Connectome

A non-parametric statistical analysis, the network-based statistics (NBSv1.2; Zalesky, 2010) was employed to perform mass univariate hypothesis testing at every (FA and NOS-weighted) connection comprising the graph to identify a weaker sub-graph

component meanwhile controlling for the family-wise error rate (FWER). A test statistic (ANCOVA, co-varied for age and gender) was computed to test for group connectivity strength differences (M=5000, $p<0.05$). Connections were threshold (T=1.5-3) to obtain a set of suprathreshold connections, namely only those connections that exceeded the set value; FWER-correction was employed regardless of the threshold choice (Zalesky et al., 2010).

Rich-club Definition & Analyses

To identify group differences in rich-club connectivity and organisation we carried out an exploratory rich-club analysis (van den Heuvel & Sporns, 2011). We investigated the contribution of FA and NOS to the rich-club coefficient and membership. A weighted rich-club coefficient (Opsahl et al., 2008) was determined by ranking nodes by their connection strength (nodal degree, W^{ranked}), thus nodes and connections were threshold to define a subgraph (W>r). Furthermore, edge weights (NOS and FA) were summed up for those connections within the subgraph and summed up again for the most highly weighted connections with rank greater than k (E>k). The ratio between W>r and E>k defined the weighted rich-club coefficient. Rich-club analysis permutation testing used a 9999 Monte Carlo resamples (R Studio v1.0.143) and FDR correction (Benjamini & Hochberg, 1995) was used to correct for 28 possible densities. Normalisation was carried out for the weighted rich-club coefficient, as φ increases as a function of k in random networks (Colizza et al., 2006). To show that rich-club nodes were more highly interconnected than chance alone, a normalised rich-club coefficient was calculated by randomly re-shuffling weights (M=500, SD<0.001, O'Donoghue et al., 2017b) while preserving network topology (Maslov & Sneppen, 2002). The number of obtained rich-club coefficients were then used to compute an empirical null

distribution of $\varphi_{random}(k)$ which was used to estimate the statistical significance of each observed measure. Hence, $\varphi_{norm}(k)$ was computed as $\varphi(k)/\varphi_{random}(k)$. Rich-club members were identified at statistically significant φ_{norm} for both diagnostic groups across a range of k, at a 60% and 70% group thresholds (O'Donoghue et al., 2017b).

Images were obtained using BrainNetViewer (https://www.nitrc.org/projects/bnv/) and NeuroMArVL (http://immersive.erc.monash.edu.au/neuromarvl/).

Results

Participants Clinical and Demographic Characteristics

Bipolar disorder participants and controls were matched for age, gender and education level attained and did not differ in age across diagnosis-by-gender subgroups ($F(3,81)=1.936$, $p=0.130$, Table 2). The majority (67.5%) of the BD group were euthymic at the time of scanning with 13 (32.5%) displaying mild anxiety and depressive signs and symptoms and all but three were medicated (Table 2). Participants with BD type I (N=34) and type II (N=6) aged 19-64 were considered in this analysis.

Whole-brain measures of integration

Global brain topological (unweighted) organization in BD was disrupted relative to controls ($F(15,67)=2.298$, $p=0.011$), Figure 2, Table 3), detected as reduced global density, degree and efficiency. When weighting these measures by either FA or NOS no difference was detected between groups (Table 3). We investigated whether lithium might be driving effects on global organization and no difference was observed for degree or strength of connectivity between on- and off-lithium BD subjects, noting that the off-lithium group may be on other mood stabilizers. Gender comparison across global measures (Table 3) showed a main effect of gender ($F(15,66)=1.829$, $p=0.049$) and a main effect of diagnosis ($F(15,66)=2.385$, $p=0.008$), but no diagnosis-by-gender interaction ($F(15,66)=1.350$, $p=0.199$). Gender differences were recorded across (FA-weighted) clustering coefficient and characteristic path length and (NOS-weighted) betweenness centrality (Table 3), the latter driven by fronto-temporo-limbic nodes in

females relative to males (*post-hoc* MANCOVA across 86 nodes, F(82,2)=0.73, p=0.74).

Permutation-based subnetwork analysis

Edge-level analysis identified a weaker subnetwork connected component (FA-weighted) for BD relative to controls (t>1.5, p=0.031) comprising 16 structural disconnections (Table 4A, Figure 3). Subcortical hypoconnectivity encompassed limbic and basal ganglia connections; specifically, edges between caudate, putamen, pallidum, hippocampus, amygdala, nucleus accumbens and several brain structures of the ventral diencephalon area (hypothalamus, mammillary bodies, subthalamic nuclei, substantia nigra and red nucleus). No significant differences were identified when NOS was employed as the edge-weight. No increased connectivity was recorded (FA and NOS-weighted) in BD. Gender comparison across FA-weighted (but not NOS) connections showed hypoconnectivity in females compared to males (t=1.5-3.5, Table 4B) for connections within basal ganglia, and between basal ganglia and limbic and temporal nodes. No hyperconnectivity was noted in females, compared to males (FA and NOS-weighted). No weaker/stronger sub-network was identified when we tested for diagnosis-by-gender interaction (FA and NOS-weighted).

Normalised Rich-club coefficient

Rich-club organization was observed for FA and NOS-weighted networks (Figure 4A), with weighted rich-club coefficient ranging from k11 to k40 possible densities, and normalised weighted coefficient from k11 to k38 densities. Across FA-weighted rich-club coefficients, we did not detect a main effect of diagnosis using permutation testing or ANCOVA (F(1,80)=0.081, p=0.777), no main effect of gender (F(1,80)=1.965,

p=0.165) or diagnosis-by-gender interaction (F(1,80)=0.070, p=0.791; Figure 4B-D). Across the range of NOS-weighted rich-club coefficients there was a main effect of diagnosis detected using permutation testing (k>30, Z=3.78, p<2.2e-16) or ANCOVA (F(1,80)=16.653, p=0.0000106), no main effect of gender (F(1,80)=0.020, p=0.888), but a diagnosis-by-gender interaction (F(1,80)=6.038, p=0.016; Figure 4B-D). Female controls had significantly lower rich-club coefficients compared to males (p=0.012), or females with BD (p=0.000016), but were not significantly different from male controls (Figures 4C).

Rich-club membership

In NOS-weighted networks (Figure 4E), rich-club membership was defined at the statistically significant network between patients and controls (k>30, Z=3.78, p<2.2e-16) after multiple comparison correction across the range of rich-club densities, for connections common to more than 60% and 70% of participants. Nodes not involved in the rich-club in BD relative to controls included fronto-limbic and posterior nodes: bilateral nucleus accumbens, and (right isthmus and rostral anterior) cingulate and left lingual gyri (Figure 4E). At a higher threshold (70%), BD membership did not involve further brain regions, namely left precuneus, bilateral medialorbitofrontal, and left superiorfrontal gyri (Figure 4E).

Clinical associations

Age of onset and illness duration did not relate to the significant graph theory measures (age of onset: r=-0.15 to 0.20, p=0.24 to 0.55; illness duration: r=-0.13 to 0.14, p=0.20 to 0.93).

Discussion

We identified impairments across whole-brain topological arrangements in BD, defined by reductions in global density, degree and efficiency. Furthermore, we observed a differentially connected subnetwork involving limbic and basal ganglia connections when accounting for the microstructural organisation of the underlying fibre bundle. We detected increased density of connections within rich-club nodes when weighting the network for streamline count, and that fronto-limbic and posterior-parietal nodes were less frequently members of BD rich-club. We did not detect differences in rich-club connectivity when weighting by the microstructural organisation of the fibre bundle. While no interaction between diagnosis and gender was evident for global or subnetwork analyses, it was clear that rich-club connectivity was driven by females with BD. Interestingly, females displayed increased whole-brain betweenness centrality relative to males, driven by fronto-temporo-limbic nodes.

In BD, overall binary topological organisation deficits were observed without weighting by any measure of the strength of the connection including lower global density, degree and efficiency relative to controls (Table 3). As degree of a node relates to the number of connections present in a network, this reduced density may directly impact global communication between regional nodes and the rest of the network (Bullmore & Sporns, 2012). Whole-brain effects revealed different arrangements of connections for BD compared to controls but not when weighting a network by FA or NOS, suggesting changes in whole-brain communication in BD may be driven by abnormalities in the brain's architectural arrangement or wiring patterns rather than in at least the examined connectivity strengths. These structural differences in BD did

not appear to relate to differences in function (cognitive measures) in an overlapping clinical sample (McPhilemy et al., 2019), suggesting that in BD this rewiring may be necessary to maintain a comparable functional outcome to that of controls.

Preserved global connectivity is consistent with two studies using a comparable tractography algorithm and edge-weight (Forde et al., 2015), and investigating connection density via measures of cortical thickness using a subject-specific parcellation (Wheeler et al., 2015). Despite evidence of preserved weighted degree and density in BD using a subject-specific cortico-subcortical mapping and NOS-weighting (Leow et al., 2013), the majority of studies to date provide network level evidence for disrupted whole-brain integration mostly defined by reduced clustering coefficient efficiency globally and longer paths and inter-hemispheric dysconnectivity (Roberts et al., 2018; Wang et al., 2018; O'Donoghue et al., 2017b; Collin et al., 2016; Gadelkarim et al., 2014; Leow et al., 2013). These abnormalities support our topological findings in BD and could relate to the inter-hemispheric dysconnectivity and reduced regional connectivity previously reported (O'Donoghue et al., 2017a).

Differences across whole-brain findings between this and other analyses are very likely to depend on different methodological approaches employed (Table 1). Topological properties of a network are largely determined and thus vary depending on the tractography algorithm used (Bastiani et al., 2012); a major strength of the present study includes non-tensor-based algorithm to reconstruct complex fibre pathways arrangements combined with a subject-specific parcellation scheme including cortical and subcortical nodes to increase anatomical meaningfulness and sensitivity of the findings. However, despite the methodological advantages of employing subject-specific node definition schemes, and crossing fibre definitions for

the edges, these methods remain approximations of true anatomical subdivisions and their connection in the brain as a network (Fornito et al., 2013).

Our findings suggest that when we consider crossing fibres in the weighting, which we posit confers increased anatomical specificity, these are not globally impaired in connectivity, in contrast to what has been previously proposed by tensor-based studies (Wang et al., 2018; Collin et al., 2016; Gadelkarim et al., 2014; Leow et al., 2013), or by those not availing of a subject-specific parcellation scheme (Roberts et al., 2018; Wang et al., 2018; O'Donoghue et al., 2017b).

Recently, nine different edge-weights were integrated into a single graph to demonstrate improvements in the characterization of patient-control differences in structural connectivity analysis, and higher sensitivity, specificity and accuracy of NOS over FA (Dimitriadis et al., 2017). This highlights a distinction between edge-weights and their utility at examining topological variance, however, further research is needed to fully understand which edge-weight may be the most biological informative estimate of anatomical connectivity. Furthermore, investigation of connectivity via both weighted and unweighted networks can inform the relationship between networks weights and topology whilst minimizing biases introduced by tractography (Fornito, 2016).

Our whole-brain effects appeared to be driven by a network of subcomponents determined statistically whereby BD showed dysconnectivity in a subnetwork involving connections between basal ganglia nuclei and between limbic nuclei as well as connections between these systems relative to controls when weighted for microstructural organisation, but unchanged when weighted by streamline count.

Though numerous volumetric and voxel-based grey and white matter neuroimaging studies have implicated these two subsystems regionally and separately in BD pathophysiology (Hibar et al., 2017, 2016; O'Donoghue et al., 2017a), we revealed changes in connectivity strength in a network involving both the basal ganglia and limbic systems. These two functionally-related subsystems appear concomitantly altered in terms of how they vary in topological arrangement in BD relative to controls and are consistent with existing regional studies. Localised dysconnectivity along with reductions in whole-brain connectivity support the hypothesis that neuroanatomical deficits of BD may be confined to specific anatomical subnetworks.

Anatomically, the striatum acts as a relay station of inputs coming from several limbic motor and sensory areas such as the amygdala, hippocampus and frontal cortex (Emsell & McDonald, 2009). Considering the functional role of these anatomical connections (Wessa et al., 2009) it is possible that these changes in connectivity strength contribute to BD emotion dysregulation. Diffusion-tensor studies have implicated the anterior limb of the internal capsule (ALIC) in BD pathophysiology (O'Donoghue et al., 2017a). This is significant considering the ALIC sits adjacent to several prominent emotion regulatory circuits forming a crucial anatomical link between the basal ganglia and the limbic system. Several white matter tracts coordinate impulses coming and leaving these two subsystems, such as the uncinate fasciculus connecting fronto-limbic structures, the ventral amygdalo-striatal tract linking basal ganglia and limbic nodes, and the fornix connecting regions belonging to the limbic system and the inferior diencephalon area. There is network level evidence of fronto-limbic dysconnectivity in BD (Ajilore et al., 2015; Forde et al., 2015; Leow et al., 2013), and comparable statistical analyses have extended fronto-limbic findings

presenting dysconnectivity across parieto-occipital connections (O'Donoghue et al., 2017b), and more recently in connections involving fronto-temporal nodes in BD (Roberts et al., 2018). Dysconnectivity within temporal networks might be a characteristic of young individuals with BD (Mean age=23.9; Roberts et al., 2018) and thus explain why we failed to detect such effect in our cohort (Mean age=42.7; Table 2).

We detected increased connection density in a rich-club involving fronto-limbic, basal ganglia and parieto-occipital connections in BD relative to controls. However, this difference was not reflected when rich-club coefficients were weighted by FA. This increase in rich-club density in BD may represent a compensatory mechanism to dysconnectivity observed in a subnetwork involving basal ganglia and limbic connections when weighted by microstructural organisation. Our findings contrast previous reports of preserved structural "backbone", or anatomical infrastructure, of BD connectome (Roberts et al., 2018; Wang et al., 2018; Collin et al., 2016). A plausible explanation for this may be the increased specificity of our connectome approach relative to other observations. Furthermore, one study has shown marginal reductions in rich-club connectivity in BD (O'Donoghue et al., 2017b), whereas two have described an increase in NOS-weighted rich-club coefficients compared to controls (Zhang et al., 2018; O'Donoghue, et al., 2016). Comparisons of rich-club findings is limited by the different rich-club network mapping employed across studies, specifically if these have confined their rich-club observations to cortical connections (Collin et al., 2016) or have not defined rich-club nodes in a subject-specific manner (Roberts et al., 2018; Wang et al., 2018 ;O'Donoghue et al., 2017b).

We cannot exclude the possibility of medication effects on our findings, though we did not detect an effect of lithium on FA and NOS strength similarly to previous investigations (O'Donoghue et al., 2017b; Collin et al., 2016), however we may have been underpowered to investigate this outcome (BD: on-lithium=13, off-lithium=27, noting that all but 3 BD on-lithium were taking other medications). Though clinically challenging, future studies should focus on medication-naïve patients and longitudinal studies after commencing or switching medication, and account for medication dosage, to rule out potential medication effects on neuroanatomical measures.

We detected differential hub involvement in BD rich-club relative to controls, with the greatest effects observed within limbic and parieto-occipital nodes. These effects were indicated by the lack of participation of the anterior and posterior portions of the cingulate gyrus, nucleus accumbens and lingual gyrus to the rich-club membership at the lower group threshold (60%). Nodes less frequently included in BD membership are consistent with neuroanatomical changes reported in the disorder (O'Donoghue et al., 2017b; Forde et al., 2015; Vederine et al., 2011; Emsell et al., 2013; Leow et al., 2013; Linke et al., 2013; Nortje et al., 2013), and anatomically overlap with brain areas involved in emotion regulation and reward – two subsystems that are of considerable interest in mood disorder pathophysiology such as BD. The cingulate cortex was not included in BD membership, which is significant considering the functional role this cortex and its projections play in cognitive and emotional processes (Emsell & McDonald, 2009). Nodes anatomically connecting with this structure, namely precuneus, medial orbitofrontal and superior frontal gyri, were also not participating in BD rich-club membership, as seen when the group threshold was increased to 70%. A 70% group threshold allows for more pathways to be compared across groups; thus

these nodes may be implicated to a lesser degree in BD relative to those that were less frequently included at 60%.

Fronto-limbic dysconnectivity is consistent with a previous membership investigation (O'Donoghue et al., 2017b), although other studies have reported preserved rich-club membership in young BD (Roberts et al., 2018) and BD with depression (Wang et al., 2018); this may suggest a differential rich-club organisation in symptomatic patients relative to patients in remission, and an age-effect on connectivity within rich-club nodes (Dennis et al., 2013). Nodes belonging to the cortico-striatal reward system, namely nucleus accumbens and medial orbitofrontal cortex were less frequently involved in BD rich-club membership relative to controls. An increase in connectivity within cortico-striatal regions has been associated with mania in BD (Damme et al., 2017). Posterior parietal and occipital nodes such as the posterior cingulate and lingual gyri, and precuneus were less frequently involved in BD membership. This finding is consistent with network analyses presenting dysconnectivity within parieto-occipital and default mode network loops in BD (Gadelkarim et al., 2014; Nortje et al., 2013; Vederine et al., 2011).

Collectively, BD is dysconnected both globally and at the highest connected subnetwork, and when defined in an anatomically precise fashion reveals the involvement of the basal ganglia in addition to fronto-limbic components. These changes were confirmed when subjects with BD type II (N=6) were removed. Further, findings were confirmed in a euthymic cohort when removing BD subjects with moderate-to-severe HDRS/HARS scores, thus they may be considered trait features of BD. These findings suggest a neuroanatomical model of BD dysconnectivity that preferentially involves communication within and between emotion regulatory and

reward-related subsystems, both independently associated with BD previously (Perry et al., 2018).

There is a degree of correspondence (85%) between nodes involved in the significant subnetwork (FA-weighted) and the rich-club members (NOS-weighted), further highlighting the distinction between edge-weights and their utility at examining brain topological variance. This was supported by a negative relationship observed between edge-weights in BD (Figure 5). Furthermore, a rich-club is not solely defined by connection-strength but also accounts for connection density.

Increased rich-club connectivity in BD appeared to be driven by the female population, though this was not the case for the significant whole-brain measures and the differently connected subcomponent. Despite evidence of modulation of structure and function within cortico-subcortical regions in BD, particularly within limbic and prefrontal nodes (Jogia et al., 2012), the effect of gender on BD neuroanatomical networks has not yet been thoroughly investigated. We observed gender differences at the whole-brain and nodal level. Lower clustering and longer paths within females' anatomical networks may relate to dysconnectivity in a subnetwork encompassing fronto-limbic, basal ganglia and temporal connections seen in females but not in males. Additionally, females exhibited higher global betweenness centrality compared to males. A positive relationship has been identified between centrality measures such as degree and betweenness centrality for highly connected nodes (Oldham et al., 2018), thus females high betweenness centrality scores may contribute to the increased rich-club connectivity seen in females with BD. Collectively, these network differences may suggest alternative pathways for communication within the female

brain, and a female-specific trade-off within networks in the direction of increased integrative capacity (high betweenness centrality) at the expense of wiring and metabolic costs (Bullmore & Sporns, 2012). Furthermore, the female brain is dependent on nodes belonging to two differently specialised subsystems for communication (highlighted by increased centrality scores, betweenness centrality and rich-club) relative to males, which may confer increased susceptibility to processes dependent on integration of emotional information in females generally, and perhaps more in females with BD. Collectively, these changes support neuroanatomical evidence of gender-specific trajectories at the human connectome level (Sun et al., 2015) and may relate to different cognitive performance seen between genders in BD (Suwalska & Łojko, 2014). Our topological findings may suggest different levels of susceptibility to BD, although further research would benefit from including further clinical measures alongside increased power to fully understand whether being female and having a diagnosis of BD leads to gender-specific connectivity changes and clinical deficits.

Conclusion

Using a graph-theoretical connectome approach we provide preliminary evidence of BD neuroanatomical dysconnectivity overlapping a subnetwork involving limbic and basal ganglia connections together and a female-driven increase in rich-club connectivity. We also report abnormalities in whole-brain integration in BD. Our findings imply a differentially dysconnected subnetwork in BD and further research should clarify the functional interplay between the two subsystems involved in relation to specific trait features of BD. This study highlights the need to account for gender differences in future analysis which may advance our understanding of any different clinical course of women and men presenting with BD. Our data support the application of non-tensor-based graph theory analyses that include cortical and subcortical brain regions defined in a subject-specific manner to optimally investigate the brains' topological arrangement and subnetwork connectivity underpinning BD, demonstrating the necessity to employ more anatomical meaningful connectome reconstructions.

Acknowledgments: This research is supported by the Irish Research Council (IRC) Postgraduate Scholarship, Ireland awarded to Leila Nabulsi, and by the Health Research Board (HRA-POR-324) awarded to Dr Dara M. Cannon. We gratefully acknowledge the participants and the support of the Wellcome-Trust HRB Clinical Research Facility and the Centre for Advanced Medical Imaging, St. James Hospital; Andrew Hoopes, Research Technician I, MGH/HST Martinos Center for Biomedical Imaging, for Freesurfer software support, Christopher Grogan, MSc, for his contribution to data processing, Jenna Pittman, BSc, and Fiona Martyn, BSc, for their contribution to data handling.

Author Disclosure Statement: No competing financial interests exist.

References

Ajilore, O., Vizueta, N., Walshaw, P., Zhan, L., Leow, A., & Altshuler, L. L. (2015). Connectome signatures of neurocognitive abnormalities in euthymic bipolar I disorder. *Journal of Psychiatric Research*, *68*, 37–44. https://doi.org/10.1016/j.jpsychires.2015.05.017

Anand, A., Li, Y., Wang, Y., Lowe, M. J., & Dzemidzic, M. (2009). Resting state corticolimbic connectivity abnormalities in unmedicated bipolar disorder and unipolar depression. *Psychiatry Research - Neuroimaging*, *171*(3), 189–198. https://doi.org/10.1016/j.pscychresns.2008.03.012

Bastiani, M., Shah, N. J., Goebel, R., & Roebroeck, A. (2012). Human cortical connectome reconstruction from diffusion weighted MRI: The effect of tractography algorithm. *NeuroImage*, *62*(3), 1732–1749. https://doi.org/https://doi.org/10.1016/j.neuroimage.2012.06.002

Benjamini, Y., & Hochberg, Y. (1995). Controlling the False Discovery Rate: A Practical and Powerful Approach to Multiple Testing. *Journal of the Royal Statistical Society. Series B (Methodological)*, *57*(1), 289–300.

Blond, B. N., Fredericks, C. A., & Blumberg, H. P. (2012). Functional neuroanatomy of bipolar disorder: Structure, function, and connectivity in an amygdala-anterior paralimbic neural system. *Bipolar Disorders*, *14*(4), 340–355. https://doi.org/10.1111/j.1399-5618.2012.01015.x

Bullmore, E., & Sporns, O. (2012). The economy of brain network organization. *Nature Reviews Neuroscience*, *13*(5), 336–349.

Chang, L. C., Jones, D. K., & Pierpaoli, C. (2005). RESTORE: Robust estimation of tensors by outlier rejection. *Magnetic Resonance in Medicine*, *53*(5), 1088–

1095. https://doi.org/10.1002/mrm.20426

Colizza, V., Flammini, A., Serrano, M. A., & Vespignani, A. (2006). Detecting rich-club ordering in complex networks. *Nature Physics*, *2*(2), 110–115. https://doi.org/10.1038/nphys209

Collin, G., van den Heuvel, M. P., Abramovic, L., Vreeker, A., de Reus, M. A., van Haren, N. E. M., Boks, M. P. M., et al. (2016). Brain network analysis reveals affected connectome structure in bipolar I disorder. *Human Brain Mapping*, *37*(1), 122–134. https://doi.org/10.1002/hbm.23017

Damme, K. S., Young, C. B., & Nusslock, R. (2017). Elevated nucleus accumbens structural connectivity associated with proneness to hypomania: A reward hypersensitivity perspective. *Social Cognitive and Affective Neuroscience*, *12*(6), 928–936. https://doi.org/10.1093/scan/nsx017

Dennis, E. L., Jahanshad, N., Toga, A. W., McMahon, K. L., Zubicaray, G. I. de, Hickie, I., Wright, M. J., et al. (2013). Development of the “rich club” in brain connectivity networks from 438 adolescents & adults aged 12 to 30. In *2013 IEEE 10th International Symposium on Biomedical Imaging* (pp. 624–627). https://doi.org/10.1109/ISBI.2013.6556552

Desikan, R. S., Ségonne, F., Fischl, B., Quinn, B. T., Dickerson, B. C., Blacker, D., Buckner, R. L., et al. (2006). An automated labeling system for subdividing the human cerebral cortex on MRI scans into gyral based regions of interest. *NeuroImage*, *31*(3), 968–980. https://doi.org/10.1016/j.neuroimage.2006.01.021

Dimitriadis, S. I., Drakesmith, M., Bells, S., Parker, G. D., Linden, D. E., & Jones, D. K. (2017). Improving the reliability of network metrics in structural brain networks by integrating different network weighting strategies into a single graph. *Frontiers in Neuroscience*, *11*(DEC), 1–17.

https://doi.org/10.3389/fnins.2017.00694

Emsell, L., Langan, C., Van Hecke, W., Barker, G. J., Leemans, A., Sunaert, S., Mccarthy, P., et al. (2013). White matter differences in euthymic bipolar I disorder: A combined magnetic resonance imaging and diffusion tensor imaging voxel-based study. *Bipolar Disorders*, *15*(4), 365–376. https://doi.org/10.1111/bdi.12073

Emsell, L., & McDonald, C. (2009). The structural neuroimaging of bipolar disorder. *International Review of Psychiatry*, *21*(4), 297–313. https://doi.org/10.1080/09540260902962081

Fischl, B. (2012). FreeSurfer. *NeuroImage*. https://doi.org/10.1016/j.neuroimage.2012.01.021

Forde, N. J., O'Donoghue, S., Scanlon, C., Emsell, L., Chaddock, C., Leemans, A., Jeurissen, B., et al. (2015). Structural brain network analysis in families multiply affected with bipolar I disorder. *Psychiatry Research - Neuroimaging*, *234*(1), 44–51. https://doi.org/10.1016/j.pscychresns.2015.08.004

Fornito, A. (2016). *Fundamentals of brain network analysis / Alex Fornito, Andrew Zalesky, Edward T. Bullmore*. (A. Zalesky & E. T. Bullmore, Eds.). Amsterdam ; Boston: Elsevier/Academic Press.

Fornito, A., Zalesky, A., & Breakspear, M. (2013). Graph analysis of the human connectome: Promise, progress, and pitfalls. *NeuroImage*, *80*(0), 426–444. https://doi.org/http://dx.doi.org/10.1016/j.neuroimage.2013.04.087

Friston, K. J. (2011). Functional and Effective Connectivity: A Review. *Brain Connectivity*, *1*(1), 13–36. https://doi.org/10.1089/brain.2011.0008

Gadelkarim, J. J., Ajilore, O., Schonfeld, D., Zhan, L., Thompson, P. M., Feusner, J. D., Kumar, A., et al. (2014). Investigating brain community structure

abnormalities in bipolar disorder using path length associated community estimation. *Human Brain Mapping*, *35*(5), 2253–2264. https://doi.org/10.1002/hbm.22324

Hallahan, B., Newell, J., Soares, J. C., Brambilla, P., Strakowski, S. M., Fleck, D. E., Kiesepp, T., et al. (2011). Structural magnetic resonance imaging in bipolar disorder: An international collaborative mega-analysis of individual adult patient data. *Biological Psychiatry*. https://doi.org/10.1016/j.biopsych.2010.08.029

Hibar, D. P., Westlye, L. T., Doan, N. T., Jahanshad, N., Cheung, J. W., Ching, C. R. K., Versace, A., et al. (2017). Cortical abnormalities in bipolar disorder: an MRI analysis of 6503 individuals from the ENIGMA Bipolar Disorder Working Group. *Molecular Psychiatry*, 1–11. https://doi.org/10.1038/mp.2017.73

Hibar, D. P., Westlye, L. T., Van Erp, T. G. M., Rasmussen, J., Leonardo, C. D., Faskowitz, J., Haukvik, U. K., et al. (2016). Subcortical volumetric abnormalities in bipolar disorder. *Molecular Psychiatry*, *21*(12), 1710–1716. https://doi.org/10.1038/mp.2015.227

Jeurissen, B., Tournier, J. D., Dhollander, T., Connelly, A., & Sijbers, J. (2014). Multi-tissue constrained spherical deconvolution for improved analysis of multi-shell diffusion MRI data. *NeuroImage*, *103*, 411–426. https://doi.org/10.1016/j.neuroimage.2014.07.061

Jogia, J., Dima, D., & Frangou, S. (2012). Sex differences in bipolar disorder: A review of neuroimaging findings and new evidence. *Bipolar Disorders*, *14*(4), 461–471. https://doi.org/10.1111/j.1399-5618.2012.01014.x

Leemans, A., Jeurissen, B., Sijbers, J., & Jones, D. (2009). ExploreDTI: a graphical toolbox for processing, analyzing, and visualizing diffusion MR data. *Proceedings 17th Scientific Meeting, International Society for Magnetic*

Resonance in Medicine, *17*(2), 3537.

Leow, A., Ajilore, O., Zhan, L., Arienzo, D., Gadelkarim, J., Zhang, A., Moody, T., et al. (2013). Impaired inter-hemispheric integration in bipolar disorder revealed with brain network analyses. *Biological Psychiatry*, *73*(2), 183–193. https://doi.org/10.1016/j.biopsych.2012.09.014

Linke, J., King, A. V., Poupon, C., Hennerici, M. G., Gass, A., & Wessa, M. (2013). Impaired anatomical connectivity and related executive functions: Differentiating vulnerability and disease marker in bipolar disorder. *Biological Psychiatry*. https://doi.org/10.1016/j.biopsych.2013.04.010

Maslov, S., & Sneppen, K. (2002). Specificity and Stability in Topology of Protein Networks. *Science*, *296*(5569), 910 LP – 913.

Mc Philemy G., Nabulsi L., Kilmartin L., O'Hora D., O'Donoghue S., TronchinG., Costello L., Najt P., Ambati S., Neilsen G., Creighton S., Byrne F., McLoughlin J., McDonaldC., Hallahan B. & Cannon D.M., (2019). Neuroanatomical Dysconnectivity Underlying Cognitive Deficits in Bipolar Disorder, *Biological Psychiatry: Cognitive Neuroscience and Neuroimaging*. https://doi.org/10.1016/j.bpsc.2019.09.004.

Merikangas, K. R., Jin, R., He, J.-P., Kessler, R. C., Lee, S., Sampson, N. A., Viana, M. C., et al. (2011). Prevalence and Correlates of Bipolar Spectrum Disorder in the World Mental Health Survey Initiative. *Archives of General Psychiatry*, *68*(3), 241–251. https://doi.org/10.1001/archgenpsychiatry.2011.12

Nortje, G., Stein, D. J., Radua, J., Mataix-Cols, D., & Horn, N. (2013). Systematic review and voxel-based meta-analysis of diffusion tensor imaging studies in bipolar disorder. *Journal of Affective Disorders*, *150*(2), 192–200. https://doi.org/10.1016/j.jad.2013.05.034

O'Donoghue, S., Forde, N.J., Sarrazin, S., Poupon, C., Houenou, J., Wessa, M., Linke, J., Philips, M.L., Versace, A., Cannon, D.M., McDonald, C. (2016). Anatomical Dysconnectivity in Bipolar 1 Disorder: A Graph Theory Study Across Three Centers. *In Proceedings of the 18th Annual Conference of the International Society for Bipolar Disorders Held Jointly with the 8th Biennial Conferece of the International Society For Affective Disorders, ISBD-ISAD 2016. Amsterdam, The Netherlands*.

O'Donoghue, S., Cannon, D. M., Perlini, C., Brambilla, P., & McDonald, C. (2015). Applying neuroimaging to detect neuroanatomical dysconnectivity in psychosis. *Epidemiology and Psychiatric Sciences*, (May), 1–5. https://doi.org/10.1017/S2045796015000074

O'Donoghue, S., Holleran, L., Cannon, D. M., & McDonald, C. (2017a). Anatomical dysconnectivity in bipolar disorder compared with schizophrenia: A selective review of structural network analyses using diffusion MRI. *Journal of Affective Disorders*, *209*, 217–228. https://doi.org/https://doi.org/10.1016/j.jad.2016.11.015

O'Donoghue, S., Kilmartin, L., O'Hora, D., Emsell, L., Langan, C., McInerney, S., Forde, N. J., et al. (2017b). Anatomical integration and rich-club connectivity in euthymic bipolar disorder. *Psychological Medicine*, 1–15. https://doi.org/10.1017/S0033291717000058

Oldham, S., Fulcher, B., Parkes, L., Arnatkeviciute, A., Suo, C., & Fornito, A. (2018). Consistency and differences between centrality metrics across distinct classes of networks. https://doi.org/10.1128/CVI.00084-09

Opsahl, T., Colizza, V., Panzarasa, P., & Ramasco, J. J. (2008). Prominence and control: The weighted rich-club effect. *Physical Review Letters*, *101*(16).

https://doi.org/10.1103/PhysRevLett.101.168702

Perry, A., Roberts, G., Mitchell, P. B., & Breakspear, M. (2018). Connectomics of bipolar disorder: a critical review, and evidence for dynamic instabilities within interoceptive networks. *Molecular Psychiatry*. https://doi.org/10.1038/s41380-018-0267-2

Roberts, G., Perry, A., Lord, A., Frankland, A., Leung, V., Holmes-Preston, E., Levy, F., et al. (2018). Structural dysconnectivity of key cognitive and emotional hubs in young people at high genetic risk for bipolar disorder. *Molecular Psychiatry*, *23*(2), 413–421. https://doi.org/10.1038/mp.2016.216

Rubinov, M., & Sporns, O. (2010). Complex network measures of brain connectivity: Uses and interpretations. *NeuroImage*, *52*(3), 1059–1069. https://doi.org/10.1016/j.neuroimage.2009.10.003

Sarwar, T., Ramamohanarao, K., & Zalesky, A. (2018). Mapping connectomes with diffusion MRI: deterministic or probabilistic tractography? *Magnetic Resonance in Medicine*, (June), 1–17. https://doi.org/10.1002/mrm.27471

Strakowski, S. M., Adler, C. M., Almeida, J., Altshuler, L. L., Blumberg, H. P., Chang, K. D., Delbello, M. P., et al. (2012). The functional neuroanatomy of bipolar disorder: A consensus model. *Bipolar Disorders*, *14*(4), 313–325. https://doi.org/10.1111/j.1399-5618.2012.01022.x

Sun, Y., Lee, R., Chen, Y., Collinson, S., Thakor, N., Bezerianos, A., & Sim, K. (2015). Progressive gender differences of structural brain networks in healthy adults: A longitudinal, diffusion tensor imaging study. *PLoS ONE*, *10*(3), 1–18. https://doi.org/10.1371/journal.pone.0118857

Suwalska, A., & Łojko, D. (2014). Sex dependence of cognitive functions in bipolar disorder. *The Scientific World Journal*, *2014*.

https://doi.org/10.1155/2014/418432

Syan, S. K., Smith, M., Frey, B. N., Remtulla, R., Kapczinski, F., Hall, G. B. C., & Minuzzi, L. (2018). Resting-state functional connectivity in individuals with bipolar disorder during clinical remission : a systematic review, 1–19. https://doi.org/10.1503/jpn.170175

Tournier, J. D., Calamante, F., & Connelly, A. (2007). Robust determination of the fibre orientation distribution in diffusion MRI: Non-negativity constrained super-resolved spherical deconvolution. *NeuroImage*, *35*(4), 1459–1472. https://doi.org/10.1016/j.neuroimage.2007.02.016

van den Heuvel, M. P., & Sporns, O. (2011). Rich-Club Organization of the Human Connectome. *Journal of Neuroscience*, *31*(44), 15775–15786. https://doi.org/10.1523/JNEUROSCI.3539-11.2011

Vederine, F. E., Wessa, M., Leboyer, M., & Houenou, J. (2011). A meta-analysis of whole-brain diffusion tensor imaging studies in bipolar disorder. *Progress in Neuro-Psychopharmacology and Biological Psychiatry*, *35*(8), 1820–1826. https://doi.org/10.1016/j.pnpbp.2011.05.009

Wang, Y., Deng, F., Jia, Y., Wang, J., Zhong, S., Huang, H., Chen, L., et al. (2018). Disrupted rich club organization and structural brain connectome in unmedicated bipolar disorder. *Psychological Medicine*, 1–9. https://doi.org/DOI: 10.1017/S0033291718001150

Wang, Y., Wang, J., Jia, Y., Zhong, S., Zhong, M., Sun, Y., Niu, M., et al. (2017). Topologically convergent and divergent functional connectivity patterns in unmedicated unipolar depression and bipolar disorder. *Translational Psychiatry*, *7*, e1165.

Wessa, M., Houenou, J., Leboyer, M., Chanraud, S., Poupon, C., Martinot, J. L., &

Paillere-Martinot, M. L. (2009). Microstructural white matter changes in euthymic bipolar patients: a whole-brain diffusion tensor imaging study. *Bipolar Disord*, *11*(8), 504–514. https://doi.org/BDI718 [pii]\r10.1111/j.1399-5618.2009.00718.x

Wheeler, A. L., Wessa, M., Szeszko, P. R., Foussias, G., Chakravarty, M. M., Lerch, J. P., DeRosse, P., et al. (2015). Further neuroimaging evidence for the deficit subtype of schizophrenia: A cortical connectomics analysis. *JAMA Psychiatry*, *72*(5), 446–455. https://doi.org/10.1001/jamapsychiatry.2014.3020

Zalesky, A., Fornito, A., & Bullmore, E. T. (2010). Network-based statistic: Identifying differences in brain networks. *NeuroImage*, *53*(4), 1197–1207. https://doi.org/10.1016/j.neuroimage.2010.06.041

Zalesky, A., Fornito, A., Cocchi, L., Gollo, L. L., van den Heuvel, M. P., & Breakspear, M. (2016). Connectome sensitivity or specificity: which is more important? *NeuroImage*, *142*, 407–420. https://doi.org/10.1016/j.neuroimage.2016.06.035

Zhang, R., Xu, R., Lu, W., Zheng, W., Miao, Q., Chen, K., Gao, Y., Bi, Y., Guan, L., So K., Lin, K. (2018). Aberrant brain structural-functional connectivity coupling in patients with bipolar disoder. In *In Proceedings of the 24th Annual Meeting of the Organisation of the Human Brain Mapping, Singapore, 2018*.

Tables Captions

Table 1: Overview of network reconstruction, weights considered and findings by today's structural connectivity studies

Table 1 Legend: No study to date has used cortico-subcortical mapping (Freesurfer) in combination with complex fibre arrangement (CSD-tractography) to investigate bipolar disorder anatomical networks. 'n.s.'=Not studied; Global=global measure; NBS=Network-based statistics; RC=Rich-club; FA=Fractional Anisotropy; NOS=Number of Streamlines; MD=Mean diffusivity; SD=Streamline Density.; CC=Clustering Coefficient; E_g=Global Efficiency; L=Path Length; DMN=Default Mode Network; ↓=decrease; ↑=increase. HC=healthy controls; BD=bipolar disorder.

Table 2: Clinical and sociodemographic details of participants

Table 2 Legend: Participants were age and gender-matched across groups. *$p<0.05$. N=13 with HDRS >7. #age of onset and illness duration are available for N=37 subjects with BD.

Table 3: Global network measures across Unweighted and Weighted networks

Table 3 Legend: Measures are shown across (i) unweighted networks, with diagnostic group differences in global density, degree and efficiency; (ii) weighted networks, with gender differences in FA-weighted clustering coefficient and characteristic path length; NOS-weighted betweenness centrality, at *$p<0.05$. Statistical comparison between diagnostic groups: MANCOVA (Wilk's Λ $F(15,67)=2.298$, $p=0.011$). Gender comparison showed (a) main effect of diagnosis (Wilk's Λ Pillai's $F(15,66)=2.385$, $p=0.008$), a (b) main effect of gender (Wilk's Λ Pillai's

F(15,66)=1.829, p=0.049) but no (c) interaction between gender and diagnosis was detected (Wilk's Λ Pillai's F(15,66)=1.350, p=0.199).

Supplemental Data

Table 4: FA-weighted subnetwork graph component showing decreased connectivity in bipolar disorder and females

Table 4 Legend: Table A and B show the set of connections comprised in the subnetwork graph component found to show a significant effect for main effect of diagnosis (A) and gender (B).

A) NBS 'T-test' (ANCOVA) co-varying for age and gender showing a weaker connected component in the bipolar group relative to controls (T>1.5, p=0.031). No statistically connected weaker subnetwork component was identified in the bipolar group at the higher thresholds tested. (i) connectivity strengths FA (A) for both groups and relative (ii) percentage decrease in strength for bipolar disorder compared to controls; (iii) the magnitude of subnetwork component difference. This network showed 2.9-8.6% reduced connection strength associated with FA-edge weighting in bipolar disorder versus control; components of the network ranged in magnitude of difference from a T>1.5 to 2.32, with the highest effects within the basal ganglia and between basal ganglia and limbic connections.

B) NBS 'T-test' (ANCOVA) co-varying for age and diagnosis, showing a weaker subnetwork graph component in the female group compared to males (T>1.5, p=0.040; T>2, p=0.036; T>3, p=0.015; T>3.5, p=0.030). Table B shows reduced connectivity associated with FA-edge weighting in females versus males; components of the network ranged in magnitude of difference from a T>1.51 to 4.07, with the highest effects within the basal ganglia and between basal ganglia and limbic connections. VentralDC=Ventral Diencephalon; HC=healthy controls; BD=bipolar disorder.

Figure 5: Relationship between edge-weights in rich-club and NBS analysis

Figure 5 Legend: NOS-weighted rich club coefficients were inversely correlated with the average FA strength of the NBS subnetwork in BD (r=-0.451, p=0.003) but not in HC (r=0.103, p=0.50). HC=healthy controls; BD=bipolar disorder.

Table 1 Overview of network reconstruction, weights and findings considered by today's structural connectivity studies

Reference	Mood-state	Structural network reconstruction						Edge-weights			Findings (BD vs HC)
		Cortical	Subcortical	AAL	FreeSurfer	DTI	CSD	Global	NBS	RC	
Leow et al., 2013	Euthymia	✓	✓	-	✓	✓	-	NOS	n.s.	n.s.	Global: ↓CC, ↓E_g, ↑L; Preserved Density or Degree
Gadelkarim et al., 2014	Euthymia	✓	-	-	✓	✓	-	n.s.	n.s.	n.s.	Global: (in-house PLACE algorithm) ≠ community structures identified in the Left posterior DMN; left-right hemispheres decoupling
Collin et al., 2016	70% Euthymia, 17% moderate-severe depression, 4% mania, 10% mixed symptoms	✓	-	-	✓	✓	-	FA, MD, SD	n.s.	FA, MD, SD	Global: ↓E_g, ↓inter-hemispheric connectivity; RC: Preserved RC connectivity; RC Edge-Analysis: preserved RC and feeder, ↓local connectivity
Forde et al., 2015	Euthymia	✓	✓	✓	-	-	✓	NOS	n.s.	n.s.	Global: preserved connectivity
O'Donoghue et al., 2017	Euthymia	✓	✓	✓	-	-	✓	FA	FA	NOS	Global: ↓CC, ↓E_g. NBS: ↓ fronto-parietal & occipital subnetwork. RC: Preserved RC connectivity; different RC membership (SFG, Thalamus)
Roberts et al., 2018	Euthymia	✓	✓	✓	-	-	✓	NOS	NOS	Binary	Global: ↑CC, ↑L. NBS: ↓rh fronto-temporal subnetwork. RC: Preserved RC connectivity; Altered RC membership; Overlap between NBS nodes and RC hubs
Wang et al., 2018	Unmedicated, depression	✓	✓	✓	-	✓	-	FA	FA	FA	Global: ↓E_g, ↑L, ↓(global)Elocal RC: Preserved RC connectivity; Preserved RC membership; RC Edge-analysis: ↓RC and feeder, preserved local connections.

Table 2 Clinical and sociodemographic details of participants

Sample	Healthy Controls	Bipolar Disorder	Statistical Comparison Between Diagnostic Groups, (U/χ2, p-value)
Number of participants	45	40	/
Age (years) Male, mean±SD Female, mean±SD	38.6±13.5 40.5±13.8 39.3±13	42.7±12.7 36.9±13.3 46.2±11.6	U=1,062, p=0.155
Gender, Male/Female (N)	21/24	20/20	X^2=0.094, p=0.759
Level of Education (SES scale) median range	6, 2-7	5, 2-7	X^2=8.249, p=0.143
Age of Onset (years)# mean±SD	-	26.1±9.5	
Illness duration (years)# mean±SD	-	16.9±10.9	
Hamilton Depression Rating Scale (HDRS) mean±SD median range	1.0±1.5 0 0-5	6.9±7.4 4.5 0-28	U=1,436, p<0.001*
Young Mania Rating Scale (YMRS) mean±SD median range	0.9±1.6 0 0-6	1.6±5.1 0.5 0-10	U=1,062, p=0.110
Hamilton Anxiety Rating Scale (HARS) mean±SD median range	0.7±1.7 0 0-8	5.0±6.5 2.5 0-27	U=1,376, p<0.001*
Medication Class (Frequency, N) Medication Naïve	/ /	3	/
Mood stabilizers Lithium only (0.4-1.2 g/day) Sodium valproate only (0.03-1.4 g/day) Lamotrigine only (0.025-0.45 g/day) Combination	- - - -	5 5 8 10	/
Antidepressants SNRI/ SSRI/NaSSA	/	7/4/4	/
Antipsychotics atypical/typical	/	30/1	/
Benzodiazepine	/	2	/
Other Psychotropic	/	7	/

Table 3 Global network measures across Unweighted and Weighted networks

	(i) Unweighted					(ii) Weighted									
						Fractional Anisotropy					Number of Streamlines				
	Healthy Controls (mean ±SD)	Bipolar Disorder (mean ±SD)	(a) Statistical Comparison Diagnosis (F, p-value)	(b) Statistical Comparison Gender (F, p-value)	(c) Interaction Gender and Diagnosis (F, p-value)	Healthy Controls (mean ±SD)	Bipolar Disorder (mean ±SD)	(a) Statistical Comparison Diagnosis (F, p-value)	(b) Statistical Comparison Gender (F, p-value)	(c) Interaction Gender and Diagnosis (F, p-value)	Healthy Controls (mean±SD)	Bipolar Disorder (mean±SD)	(a) Statistical Comparison Diagnosis (F, p-value)	(b) Statistical Comparison Gender (F, p-value)	(c) Interaction Gender and Diagnosis (F, p-value)
Density **Male** **Female**	0.36±0.03 0.36±0.03 0.36±0.03	0.34±0.03 0.34±0.03 0.34±0.03	4.22, 0.04*	0.20, 0.66	0.08, 0.77	-	-	-	-	-	-	-	-	-	-
Degree **Male** **Female**	30.15±2.64 30.15±2.58 30.16±2.75	28.94±2.24 29.22±1.89 28.66±2.57	4.22, 0.04*	0.20, 0.66	0.08, 0.77	-	-	-	-	-	-	-	-	-	-
Strength **Male** **Female**	-	-	-	-	-	10.32±1.61 10.50±1.29 10.17±1.86	9.85±1.16 10.16±0.82 9.53±1.36	1.932, 0.168	2.26, 0.14	0.06, 0.81	2013.86±273.44 1983.12±260.61 2040.75±287.00	1926.22±285.41 1974.53±304.44 1877.91±263.84	0.83, 0.37	0.01, 0.92	0.33, p=0.57
Clustering Coefficient **Male** **Female**	0.64±0.02 0.64±0.02 0.64±0.02	0.63±0.02 0.64±0.02 0.63±0.02	3.27, 0.07	1.63, 0.21	0.58, 0.45	0.21±0.03 0.22±0.02 0.21±0.03	0.21±0.02 0.21±0.01 0.20±0.02	0.367, 0.546	5.11, 0.03*	0.05, 0.83	24.31±4.74 23.22±3.35 25.25±5.58	23.73±3.91 23.99±3.70 23.48±4.19	0.02, 0.89	0.99, 0.32	0.71, p=0.40
Characteristic Path Length **Male** **Female**	1.69±0.05 1.69±0.05 1.70±0.06	1.71±0.05 1.70±0.03 1.72±0.06	2.22, 0.14	1.51, 0.22	0.03, 0.86	4.56±0.54 4.41±0.52 4.68±0.83	4.59±0.47 4.45±0.23 4.72±0.60	0.015, 0.904	4.13, 0.05*	0.04, 0.85	0.02±0.01 0.02±0.01 0.02±0.01	0.02±0.01 0.02±0.01 0.02±0.01	0.13, 0.72	0.25, 0.62	1.55, p=0.22
Global Efficiency **Male** **Female**	0.66±0.03 0.66±0.03 0.67±0.02	0.65±0.03 0.65±0.03 0.65±0.03	4.86, 0.03*	0.29, 0.59	0.59, 0.45	0.25±0.03 0.25±0.02 0.24±0.03	0.24±0.02 0.25±0.01 0.24±0.02	1.012, 0.317	2.36, 0.12	0.04, 0.84	95.90±13.68 93.93±12.90 97.64±14.38	92.61±13.88 95.27±14.34 89.95±13.22	0.36, 0.55	0.01, 0.94	836, p=0.36
Betweenness Centrality **Male** **Female**	58.08±4.65 57.06±3.99 58.98±5.07	58.98±4.14 58.05±2.76 59.91±5.07	0.74, 0.39	3.72, 0.06	0.05, 0.83	78.29±5.79 77.98±6.54 78.56±5.18	79.25±7.67 76.81±6.48 81.70±8.13	0.322, 0.572	3.44, 0.07	1.79, 0.16	144.82±13.41 140.40±10.53 148.68±14.63	146.45±12.56 144.23±8.89 148.66±15.38	0.52, 0.47	5.28, 0.02*	0.39, p=0.53

1. Cortico-subcortical mapping (FreeSurfer)
Structural T1-weighted MRI Scan
2. Deterministic (non-tensor) constrained spherical deconvolution (CSD) tractography
Diffusion-weighted MRI Scan
3. Connectivity matrices
(i)
(ii)
(iii)
(i) Binary, (ii) FA, (iii) NOS
4. Global Network Measures
Nodes = Grey matter regions
Edges = White matter pathways
5. Network-based statistics
= sub-network component
6. Rich-Club
= rich-club brain region (node)
= non rich-club node
= non rich-club white matter connection (edge)
= rich-club white matter edge

Figure 1

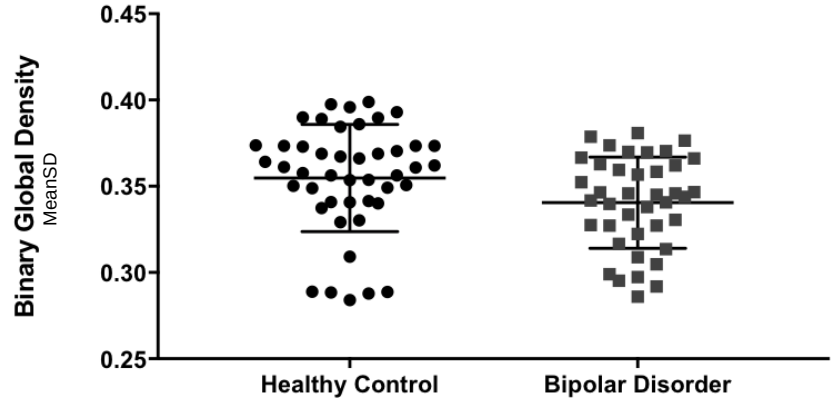
Binary Global Density
MeanSD
0.45
0.40
0.35
0.30
0.25
Healthy Control
Bipolar Disorder

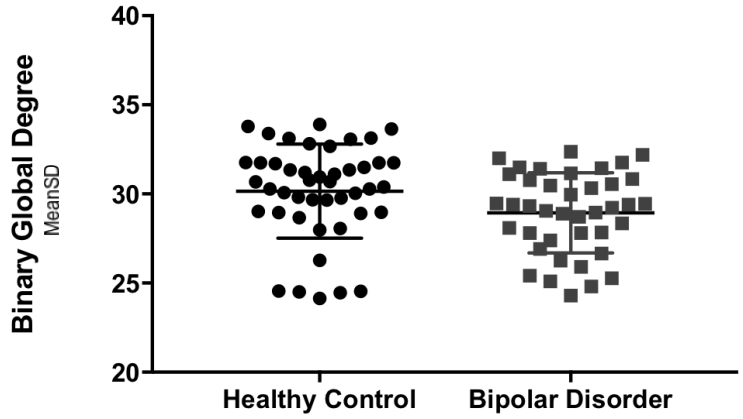
Binary Global Degree
MeanSD
40
35
30
25
20
Healthy Control
Bipolar Disorder

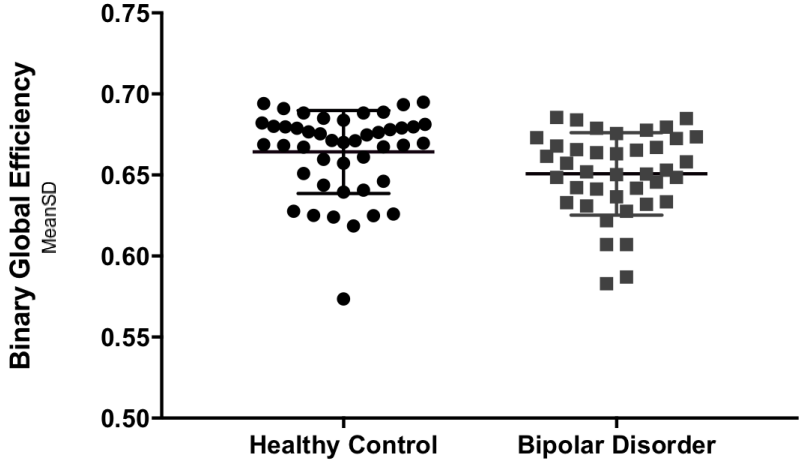
Binary Global Efficiency
MeanSD
0.75
0.70
0.65
0.60
0.55
0.50
Healthy Control
Bipolar Disorder

Figure 2

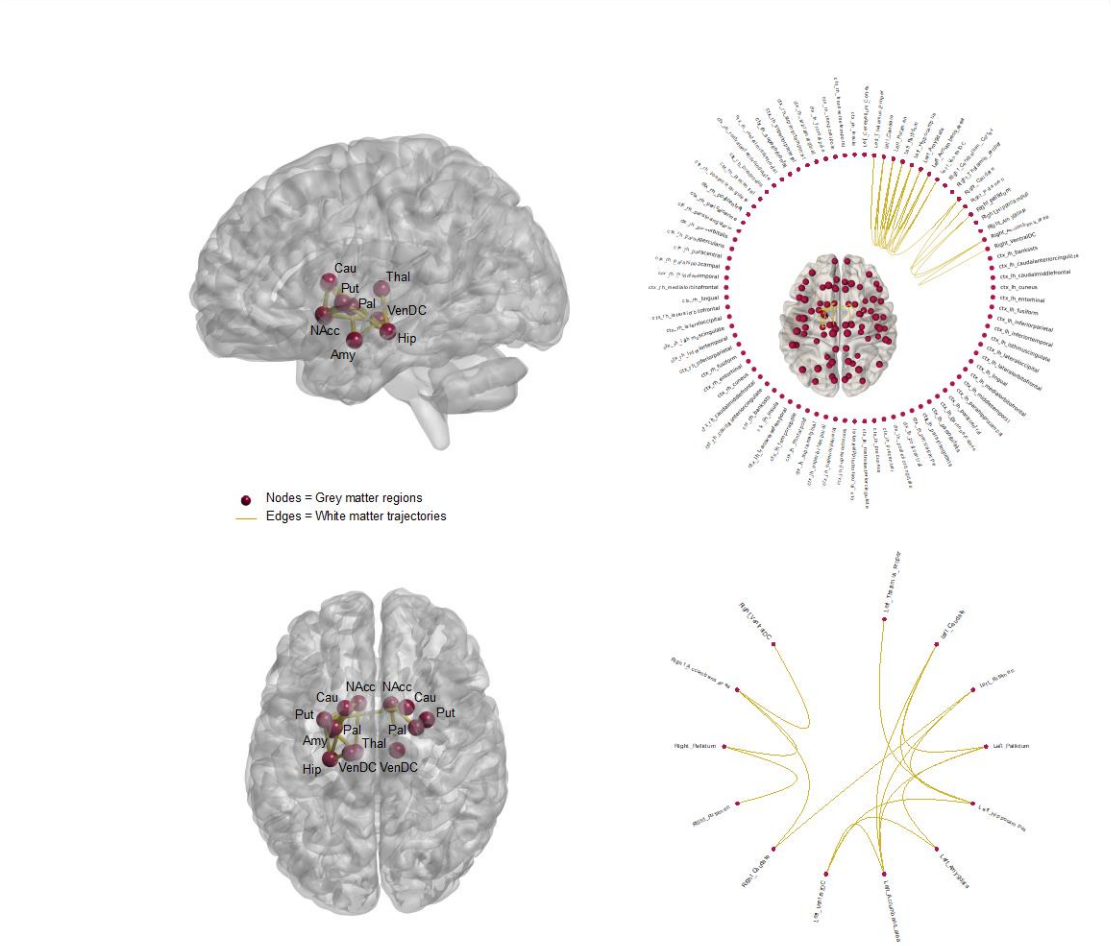
Cau
Thal
Put
Pal
VenDC
NAcc
Hip
Amy
Nodes = Grey matter regions
Edges = White matter trajectories
NAcc
NAcc
Cau
Cau
Put
Put
Pal
Pal
Amy
Thal
Hip
VenDC
VenDC

Figure 3

A

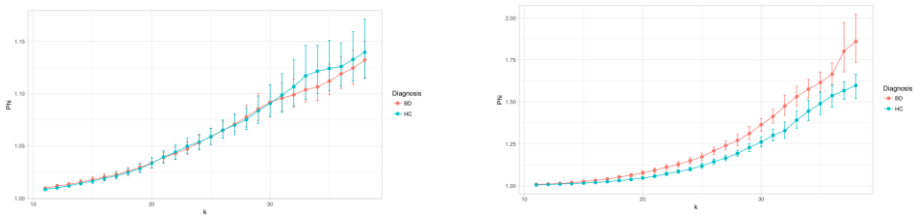

B

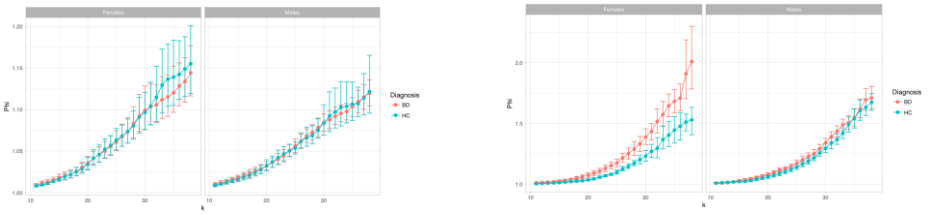

C

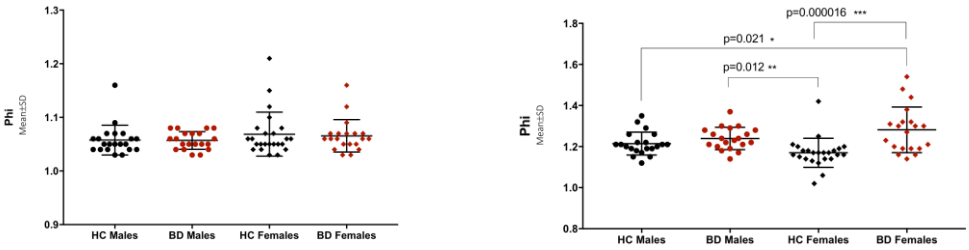

D

	Fractional Anisotropy			Number of streamlines		
	Healthy Controls (mean±SD)	Bipolar Disorder (mean±SD)	Statistical comparison (F, p-value)	Healthy Controls (mean±SD)	Bipolar Disorder (mean±SD)	Statistical comparison (F, p-value)
Overall Phi	1.06±0.36	1.06±0.24	No difference detected§	1.19±0.07	1.26±0.09	k>30, Z=3.78, p<2.2e-16§
Male	1.058±0.03	1.06±0.02	0.070, 0.791	1.21±0.02	1.24±0.02	6.038, 0.016*
Female	1.07±0.04	1.07±0.03		1.17±0.02	1.28±0.02	

E

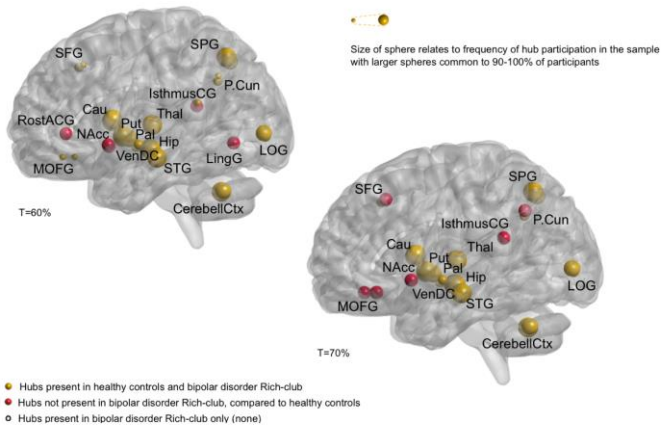

Figure 4

Figures Captions

Figure 1: Human connectome reconstruction

Figure 1 Legend: (1) Brain region definition into 34 cortical and 18 subcortical - FreeSurfer v5.3.0; (2) White matter trajectories - ExploreDTI v4.8.6; (3) Connectivity matrices – ExploreDTI v4.8.6; (4) Global network measures – Brain Connectivity Toolbox v1.52; (5) Network Based Statistics, NBS v1.2; (6) Rich-Club analysis – Brain Connectivity Toolbox v1.52, Rstudio v1.0.14.

Figure 2: Global network measures affected in bipolar disorder

Figure 2 Legend: Bipolar disorder group exhibited greater dysconnectivity compared to healthy controls across unweighted networks. Dysconnectivity was defined by reduced global density, degree and global efficiency. Bars represent Mean±SD.

Figure 3: FA-weighted subnetwork graph component showing decreased connectivity in bipolar disorder

Figure 3 Legend: This network showed reduced connection strength associated with FA-edge weighting in bipolar disorder versus control, with the highest effects within the basal ganglia and between basal ganglia and limbic connections (T>1.5, p=0.031). VentralDC=Ventral Diencephalon; ctx=Cortex.

Figure 4: Normalised Rich-club coefficients (Phi) and Gender

Figure 4 Legend: FA-weighted coefficients (left) and NOS-weighted coefficients (right). (a) Rich-club curves across k densities 11-38 for BD (red) and HC (blue), with bootstrap 95%CI. (b) Normalised rich-club coefficient values across k densities 11-38, split by gender for BD (red) and HC (blue); bars represent bootstrap 95%CI. (c)

Normalised rich-club coefficients plotted for gender and diagnostic group; bars represent Mean±SD. In NOS, but not in FA, females BD showed increased rich-club coefficients compared to female and male HC; in addition, female HC showed lower rich-club coefficients compared to males BD (*post-hoc* Tukey's). *p<0.05. (d) Statistical comparison of normalised rich-club coefficient across diagnostic groups and gender. §permutation test: 9999 Monte Carlo resamples (FDR-corrected). In NOS, but not in FA, rich-club connectivity was significantly different for BD group (k>30 Z=3.78, p<2.2e-16, compared to HC. (e) NOS-weighted rich-club membership. Nodes in yellow represent rich-club hubs common to all healthy volunteers. Nodes in red represent rich-club hubs less frequently involved in bipolar disorder. The size of the nodes relates to rich-club hubs common to participants within the bipolar disorder group, with larger spheres being common to 80-100% of participants.